

## Polarization effects and charge transfer in the KcsA potassium channel

Denis Bucher<sup>a</sup>, Simone Raugei<sup>b</sup>, Leonardo Guidoni<sup>a,c</sup>, Matteo Dal Peraro<sup>d</sup>,  
Ursula Rothlisberger<sup>a</sup>, Paolo Carloni<sup>b,\*</sup>, Michael L. Klein<sup>d</sup>

<sup>a</sup> *École Polytechnique Fédérale de Lausanne EPFL, Institute of Chemical Sciences and Engineering, CH-1015 Lausanne, Switzerland*

<sup>b</sup> *International School for Advanced Studies, SISSA-ISAS and INFN-Democritos Center, via Beirut 4, 34014 Trieste, Italy*

<sup>c</sup> *University of Rome “La Sapienza” and INFN, Physics Department, P.le A. Moro 5, 00185 Roma, Italy*

<sup>d</sup> *Center for Molecular Modeling, University of Pennsylvania 231 South 34th Street, Philadelphia, PA 19104, USA*

Received 7 February 2006; received in revised form 18 April 2006; accepted 18 April 2006

Available online 26 April 2006

### Abstract

The electronic structure of the selectivity filter of KcsA K<sup>+</sup> channel is investigated by density functional theory (DFT/BLYP) and QM/MM methods. The quantum part includes the selectivity filter, which is polarized by the electrostatic field of the environment treated with the Amber force field. The details of the electronic structure were investigated using the maximally localized Wannier function centers of charge and Bader's atoms in molecules charge analysis. Our results show that the channel backbone carbonyl groups are largely polarized and that there is a sizeable charge transfer from the backbone to the cations. These effects are expected to be important for an accurate description of the carbonyl groups and the ion–ion electrostatic repulsion, which have been proposed to play a central role for the selectivity mechanism of the channel [S.Y. Noskov, S. Berneche, B. Roux, Control of ion selectivity in potassium channels by electrostatic and dynamic properties of carbonyl ligands. *Nature* 431 (2004) 830–834].

© 2006 Elsevier B.V. All rights reserved.

**Keywords:** Potassium channel; Polarization effects; KcsA; Charge transfer; Wannier centers; Bader charge; First principles molecular dynamics

### 1. Introduction

Potassium channels play a key role for maintaining a suitable ionic balance across cell membranes and for generating electrical signals in a variety of processes, including neuron communication, heart beat and insulin release [1,2]. Central to the function of these proteins is the ability of such channels to support transmembrane ion conduction at nearly diffusion-limited rates ( $\sim 10^7$  ions s<sup>-1</sup> channel<sup>-1</sup>) while discriminating for K<sup>+</sup> over Na<sup>+</sup> [2].

The availability of structural information about the KcsA K<sup>+</sup> potassium channel from *Streptomyces lividians* in different conditions of permeant cation and ionic concentrations [3,4] provides the opportunity to gain a detailed understanding of ion selectivity. Because all of the K<sup>+</sup> channels (including

voltage-gated K<sup>+</sup> channels [5]), share the same core structure [3,4], the conclusion drawn on this channel are expected to be generally valid.

The KcsA K<sup>+</sup> channel is a tetramer. Each subunit contains two transmembrane helices (M1 and M2) with an intervening loop formed by a short helix (P-loop, Fig. 1a). The machinery responsible for ion selectivity is the so-called selectivity filter, which features the conserved TVGYG signature [6,7]. The filter is located at the narrowest region of the pore, close to the outer mouth of the channel (Fig. 1b), and it is paved with carbonyl groups that form four binding sites generally occupied, at physiological conditions (160mM K<sup>+</sup>), by two monovalent cations and two water molecules.

Permeation is thought to occur through a concerted motion of potassium and water within the pore using the so-called “knock-on” mechanism [8]. The timescale of the K<sup>+</sup> translocation under typical transmembrane potentials is of the order of 10–20 ns [9]. In the most common scenario, one water molecule per K<sup>+</sup> ion is transported through the pore. This vision is confirmed both by

\* Corresponding author.

E-mail address: carloni@sissa.it (P. Carloni).

experiments [10] and molecular dynamics simulations (MD) [11–13].

The ion selectivity has been investigated by MD and free energy calculations. Although in principle this property cannot be completely explained without taking into account both equilibrium and non-equilibrium effects of the ion current, such computational approaches have turned out to provide a proper description of the conduction process, allowing one to identify spontaneous [13–16] and activated [11,17–19] pathways through the selectivity filter of varying complexity, involving different number of loading states. In particular, (i) free energy calculations [11–13,18–20,73] on the different binding sites of the filter also showed excellent agreement with the available experimental measure of selectivity ( $\Delta\Delta G=5\text{--}6\text{ kcal/mol}$ ) [21,22]. Based on these calculations, the (1010) and (0101) states of the filter, in which the  $\text{K}^+$  ions are located, respectively, at the  $\text{S}_1$ ,  $\text{S}_3$  and  $\text{S}_2$ ,  $\text{S}_4$  sites, were found to be the most stable. (ii) Considering that a purely geometrically based operating mechanism could not completely explain the selectivity process, Roux and co-workers have put forward the idea that the local electrostatic and dynamical properties play a key role for selectivity [23,24]. The balance between attractive and repulsive forces in the filter, such as the carbonyl–carbonyl electrostatic repulsion, and the core repulsions of ions and protein–ion interactions, determine the pore width and the ability of the ligands to readjust to the ion size dynamically. In this respect, molecular dynamics (MD) simulations showed a considerable degree of flexibility of the filter: the average thermal fluctuation of the  $\alpha$ -carbons of the filter is  $\sim 0.5\text{ \AA}$  [23,24].

Obviously, an accurate force field is crucial to be able to make predictions about ion permeation and selectivity. As discussed recently by Roux and Berneche [25], the development of force fields has not yet reached a point where it can produce accurate results for relative free energies in all cases. In addition to parameterization and transferability issues, which can be raised in any force field-based calculation, the presence of high electric fields in the  $\text{K}^+$  channels gives rise to *induced polarization* effects that can modify the picture of ion conduction drawn up by non-polarizable force fields. For instance, three ion filling states of the filter are only 5–15 kcal/mol less stable than the more common two ion filling states [18] and could possibly be stabilized by including polarization effects. Another significant effect that may be at the core of the selectivity mechanism is the screening of the ion–ion repulsion interaction through the polarization of the carbonyl ligands. All of these effects cannot be taken into account with standard non-polarizable force fields. It appears therefore crucial to include polarization effects into the parameterization of force fields [26,27]. In fact, although the mean field treatment of polarization often provides an agreement with experimental data, recent reports have suggested shortcomings in the non-polarizable force field descriptions [28,29]. This realization is driving toward the development of a new class of polarizable force fields [26,30–37].

In addition, *charge transfer* effects might also play a role. In a previous study on charge transfer at the ion/solvent interface [38], it was found that  $\text{K}^+$  and  $\text{Na}^+$  cations withdraw a small, yet significant, fraction of electronic charge from the solvent, and give rise to a pure electrostatic polarization of the solvating

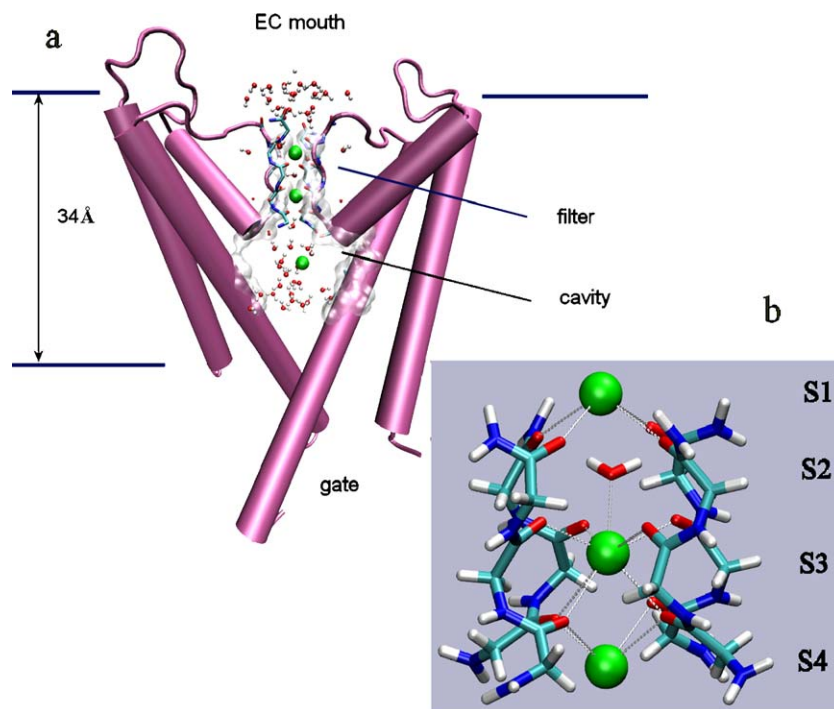


Fig. 1. Schematic diagram of the KcsA  $\text{K}^+$  channel [41]: (a) Only two of the symmetry equivalent subunits are shown along with the ions in the filter cavity and the approximate location of the lipid bilayer (EC mouth=Extra-Cellular mouth); (b) Selectivity filter with the position of the ( $\text{S}_1\text{--}\text{S}_4$ ) binding sites indicated. The occupation (1011) is shown.

water molecules. A quantification of induced polarization and charge transfer effects in ion channels and their impact on the selectivity mechanism however has yet to be established [38,39].

Herein, we examine polarization effects and charge transfer in the  $K^+$  KcsA channel by performing MD simulations followed by a mixed quantum mechanical (QM)/classical mechanical (MM) study in which the filter region is treated at the density functional theory (DFT) level [40] and the rest of the protein with the AMBER force field [14,15]. In this way the induced polarization and charge transfer effects can be analyzed in detail. In particular, we focus our analysis on the electronic density response of the protein backbone to the presence of ions inside the filter during the hopping process of an ion from the  $S_3$  to the  $S_2$  binding site.

## 2. Methods

The MD and QM/MM calculations are based on the KcsA  $K^+$  channel protein structure of Zhou et al. (pdb code: 1K4C) [41] immersed in an equilibrated water–*n*-octane ( $73.6 \times 73 \times 73$ ) $\text{\AA}^3$  box. This approach supplies a stable hydrophilic–hydrophobic liquid interface quickly adaptable to the protein and has been previously applied to transmembrane channel models [42] and KcsA [14,15]. As in previous works, the water–hydrocarbon interface is located between Trp-87 and Thr-85 (extracellular side) and between Trp-113 and Arg-117 (intracellular side). This choice, suggested by Doyle et al. [43], is in good agreement with EPR data [44]. The selectivity filter at the start of the simulation was occupied by ions in ( $S_1, S_3$ ) binding sites, (1010) hereafter using the notation introduced by Aqvist [11] (see Fig. 1).

The classical MD simulations were carried out using the AMBER 7.0 suite of programs (Amber/parm94 force field) [45]. Periodic boundary conditions were applied and electrostatic interactions were calculated using the particle mesh Ewald summation (PME) [46]. First, energy minimization was carried out using 1000 steps of a steepest descent algorithm until a rms gradient of  $5 \cdot 10^{-5}$  kcal/mol/ $\text{\AA}$  was reached. Next, a 0.2 ns MD dynamics was performed with the protein backbone and the cation positions restrained. Then, after this equilibration period, free MD simulations were performed in the NVT ensemble for 0.5 ns. Temperature scaling was used, at 300 K, with a time constant for heat bath coupling of 1 ps. A cutoff was used for long-range interactions: 10  $\text{\AA}$  for van der Waals interactions and 12  $\text{\AA}$  for the real space part of the electrostatic interactions. Simulations with both  $K^+$  and  $Na^+$  inside the selectivity filter were performed. During the classical MD simulation, the (1011) state [47,48] (Fig. 1) occurred after 0.2 ns. This state in turn evolved in 5 ps into the (1 0101) state.

QM/MM simulations, based on the (1010) and (1011) states as obtained by MD calculations, were carried out within DFT-based Car–Parrinello [49] molecular dynamics/MM dynamics scheme as implemented in the CPMD code [50]. The QM simulation box included the residues Gly-77, Val-76, Thr-75, 2 water molecules, and, depending on the starting state, 2 or 3 selectivity filter  $K^+$  ions, i.e. a total of 105 or 106 QM atoms

enclosed in a  $22 \times 22 \times 20$   $\text{\AA}$  quantum box. The quantum problem was solved using the gradient corrected Becke exchange [51,52] and the Lee, Parr and Yang correlation functionals [51,52]. The core–valence electron interactions were described using Martins and Trouiller pseudopotentials [53]. The Kohn–Sham orbitals were expanded in a plane wave (PW) basis set up to an energy cutoff of 70 Ry. The electronic wave functions were optimized up to changes in the Kohn–Sham energy lower than 0.0006 kcal/mol. The time step for the dynamics was 0.097 fs, which allowed us to employ a fictitious electron mass for the Car–Parrinello dynamics of 600 a.u. The AMBER/parm94 force field was used for the MM part of the QM/MM simulations. Capping hydrogen atoms were used to complete the valence of the QM/MM boundary atoms. An equilibrium classical configuration of the (1010) state was first re-equilibrated for 2 ps at 300 K, and the trajectory was then sampled for further 2 ps. The unstable (1011) state configuration was instead re-equilibrated at 300 K for few hundreds of femtoseconds keeping the selectivity filter atoms fixed. Then, the system was left free to evolve at 300 K. The temperature was kept constant using a Nose–Hoover chain of thermostats [54,55] with a coupling constant of 700  $\text{cm}^{-1}$ . To test the accuracy of the adopted QM calculations, the elementary interaction energy of a  $K^+$  and of a  $Na^+$  with the two most significant molecular moieties in the present system, i.e. a water molecule and a backbone carbonyl (represented as *N*-methyl acetamide), was also calculated. As can be seen from Table 1, the values obtained in the present study agree well with previously reported data.

The electronic structure was then analyzed in terms of: (i) Wannier functions, (ii) local dipole moments of cations and ligands and (iii) atoms in molecules analysis on the electronic structure calculations obtained from the QM/MM simulations.

Maximally localized Wannier orbitals [56] (WO's) were calculated on 20 equispaced (in time) configurations extracted from the two sets of QM/MM simulations that were performed. Since the full information contained in the Wannier orbitals is difficult to represent, only the centers of charge of the Wannier functions, the so-called Wannier Function Centers (WFCs) [56], were monitored. A WFC analysis was performed on each snapshot after reoptimizing the wavefunction using a PW cutoff of 80 Ry. The electronic response of the filter to the presence of

Table 1

Calculated and experimental (last row) elementary interaction energy of a  $K^+$  and of a  $Na^+$  with the two most significant molecular moieties in the present system: a water molecule and a backbone carbonyl (represented as *N*-methyl acetamide, NMA)

| $K^+$     |           | $Na^+$    |           |   |
|-----------|-----------|-----------|-----------|---|
| Water     | NMA       | Water     | NMA       |   |
| 16.1      | 26.0      | 22.9      | 35.3      | DFT/BLYP with pseudopotentials (present study)  |
| 15.9–17.6 | 24.8–31.7 | 24.0–25.8 | 38.4–40.4 | Ab-initio (Hartree–Fock level, Ref. [69])       |
| 17.6–18.9 | 16.8–24.1 | 22.8–26.3 | 20.6–30.1 | Empirical force fields (Refs. [11,13,15,20,70]) |
| 17.9      | 28.3–32.3 | 24.0      | 33.7–39.0 | Experimental values (Refs. [71,72])             |

the ions was then computed comparing the WFC to the corresponding reference state in which the  $S_3$  ion was removed while leaving all of the other atoms fixed. In this way, the induced polarization effects due to specific ions could be quantified by the displacement of the WFC. Local dipole moments on the carbonyl ligands were also calculated according to the procedure used in Ref [56]. These dipoles were compared with that of formamide in vacuo.<sup>1</sup>

Charge transfer was analyzed using Bader's atoms in molecules (AIM) approach [57]. The analysis was performed on the same two 20 frame-sets used for the WFC analysis. While for the WFC analysis the size of the cell was large enough to have converged values, in this case it was deemed necessary to enlarge the QM region in order to have converged charges (i.e. not dependent on the size of the simulation cell). The simulation box we used was obtained by enlarging the original one including also the Tyr-78 and Gly-79 residues and 5 water molecules at the inner and outer part of the selectivity filter (resulting in a total of 197 atoms enclosed in a QM box of  $26.5 \times 26.5 \times 38.1 \text{ \AA}$ ); the positions of the extra atoms added were not relaxed. Also in this case, the wavefunctions were reoptimized using a PW cutoff of 80Ry. Enlarging the simulation cell further does not alter the atomic charges of the inner part of the selectivity filter. AIM atomic charges were obtained by direct integration of the molecular electronic density of particular subsystems divided by zero flux surfaces. AIM gives a rigorous physical criterion to identify molecular surfaces in super molecular clusters or in the condensed phase, and seems to have very little basis set dependency [58]. In addition, electrostatic moments derived from AIM result in rapidly convergent multipole expansions of electrostatic potentials [59,60]. Finally, due to the use of a PW basis set, the results are not affected by the basis set super position error (BSSE), which could give rise to a fictitious charge transfer [61].

### 3. Results

#### 3.1. Structural features

In its standard state, the selectivity filter is occupied by two  $K^+$  ions in alternate binding sites with a water molecule in between [48]. The cavity at the bottom of the selectivity filter and the extra-cellular side are also occupied with one ion [62], which is typically 5–7-fold coordinated by the water molecules in the inner cavity. Inside the selectivity filter,  $K^+$  ions are usually 8-fold coordinated by the carbonyl ligands and can be additionally coordinated to a water molecule at a slightly longer distance [63].

Classical MD simulations were carried out, followed by QM/MM calculations. After 0.2 ns, classical MD simulations in the initial (1010) state, the system evolved to the (1011) state (Fig. 1b), and in turn after 5 ps to the (0101) state obtained by pushing an ion toward the extra-cellular side of the channel. This state

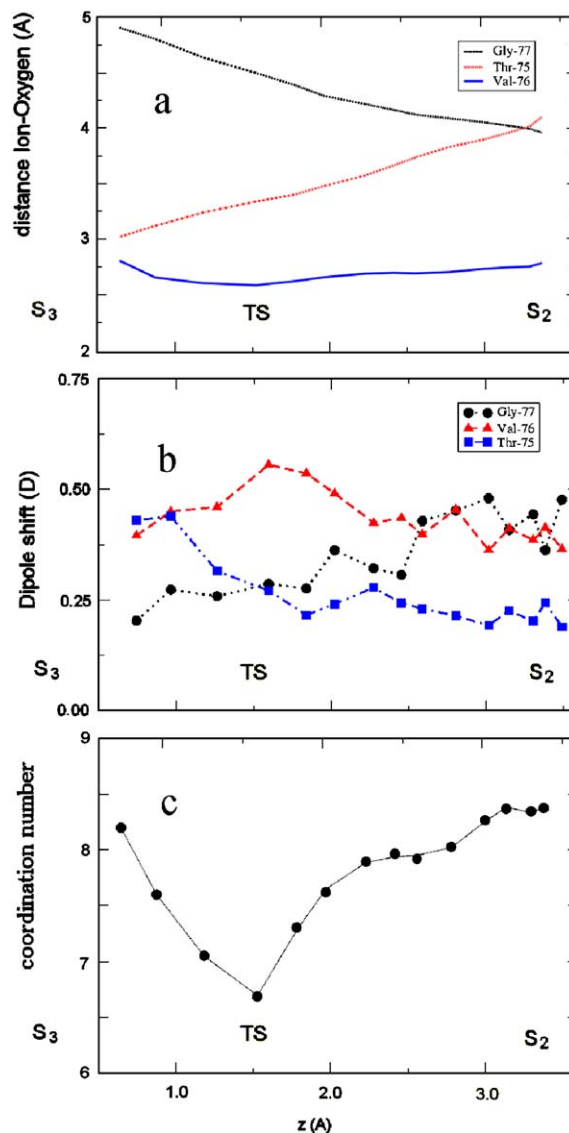


Fig. 2. Structural and electronic properties during the translocation process of  $K^+$  from binding site  $S_3$  to  $S_2$ . In all of the graphs the abscissa represents the vertical position of the ion relative to the  $S_3$  binding site. (a) Distances between the  $K^+$  ion and residues of the filter Gly-77, Val-76, Thr-75. (b) Evolution of C=O dipole (relative to formamide) on Gly-77, Val-76, Thr-75. (c)  $K^+$  coordination number.

remained for another 0.3 ns. Two QM/MM simulations were run after 0.2 ns of classical simulation (1010 state) and after the appearance of the (1011) state. To provide qualitative insight on the electronic structure change upon replacement of  $K^+$  with  $Na^+$ , we have performed calculations on QM/MM snapshots in which  $K^+$  at  $S_3$  has been replaced with  $Na^+$ .

##### 3.1.1. (1010) state

Although MD-averages were calculated for all the properties presented here, we are aware that the very short timescale prevents us to obtain fully converged quantities. More extended QM/MM simulations are in progress to check the degree of convergence of the results reported here. According to reference data for ion/ligand interactions [29] and previous work on KcsA

<sup>1</sup> The experimental dipole moment of formamide (2.7 D) is well reproduced using the BLYP functional (2.75 D).

[63], we considered an O atom to be coordinated to a cation if the distance of the  $K^+$ –O distance is smaller than 3.2 Å. 7–8 oxygens are found in the coordination shell of  $K^+$ . The average K–O distance for the  $S_1$  and  $S_3$  binding sites is 2.8 Å with a standard mean deviation of 0.3 Å. Similar distances are reported in classical MD ( $2.9 \text{ Å} \pm 0.3$ ) [63] and are within the range expected from analysis of simple inorganic crystals (2.67–3.22 Å) [29].

### 3.1.2. (1011) state

As in the classical MD, the system evolved within few picoseconds to a (0101) state by pushing an ion toward the extra-cellular side of the channel. We further note that as the  $K^+$  at  $S_3$  moves across the transition state, it gets closer to the Gly-77 carbonyl rings and further apart from the carbonyl ring formed by the four Thr-75 residues. The cation remains however tightly bound to the Val-76 carbonyls (Fig. 2a). In the transition state between the binding sites  $S_2$  and  $S_3$ , the ion is 4-fold coordinated to the Val-76 ring and only remotely coordinated to two additional carbonyl ligands of the upper or lower ring (Fig. 2c).

### 3.2. Polarization effects

Effects related to the polarization of the electronic structure were analyzed in terms of the local dipole moments of carbonyl ligands. The calculation was performed on snapshots extracted from an equilibrium QM/MM simulation of the (1010) state.

The calculated local dipole moments show a broad distribution (Fig. 3, top left panel) and they are, on average, 0.2D greater than the carbonyl local dipole moment of formamide in vacuo. The replacement of  $K^+$  in  $S_3$  with  $Na^+$  produces a much larger polarization, the local dipole moment being 1.5D larger than that in formamide (Fig. 3, top, right panel). This value is probably underestimated as the calculation of the dipole moment in the presence of  $Na^+$  was performed keeping the geometry obtained with the  $K^+$  ion at  $S_3$ . Since the Na–O distance in the energy-minimized configuration is significantly shorter, the polarization effects will be larger, as already noticed in Ref. [63]. In contrast, the dipole on Val-76 computed without the  $S_3$  ion and keeping the same structure of the filled  $S_3$  site (Fig. 3, top, right panel) is 0.64D smaller than the dipole of formamide in the gas phase. Thus, the direct consequence of the electrostatic repulsion between the carbonyls [64] is to induce a strong displacement of the electronic cloud.

The relaxation of the filter due to carbonyl–carbonyl repulsion was investigated via QM/MM trajectory spanning a few hundred femtoseconds, after removing the  $K^+$  ion in the  $S_3$  binding site. A second short simulation was also performed substituting  $Na^+$  in the  $S_3$  binding site. In the latter, the filter geometry relaxed very quickly around the cation. Although these simulations are very short, they confirm that, even when including the polarization effects, the carbonyl–carbonyl repulsion has probably little effect on the pore radius, as opposed to the ion–carbonyl interaction [64]. Taken at face value, these findings suggest an even stronger polarization

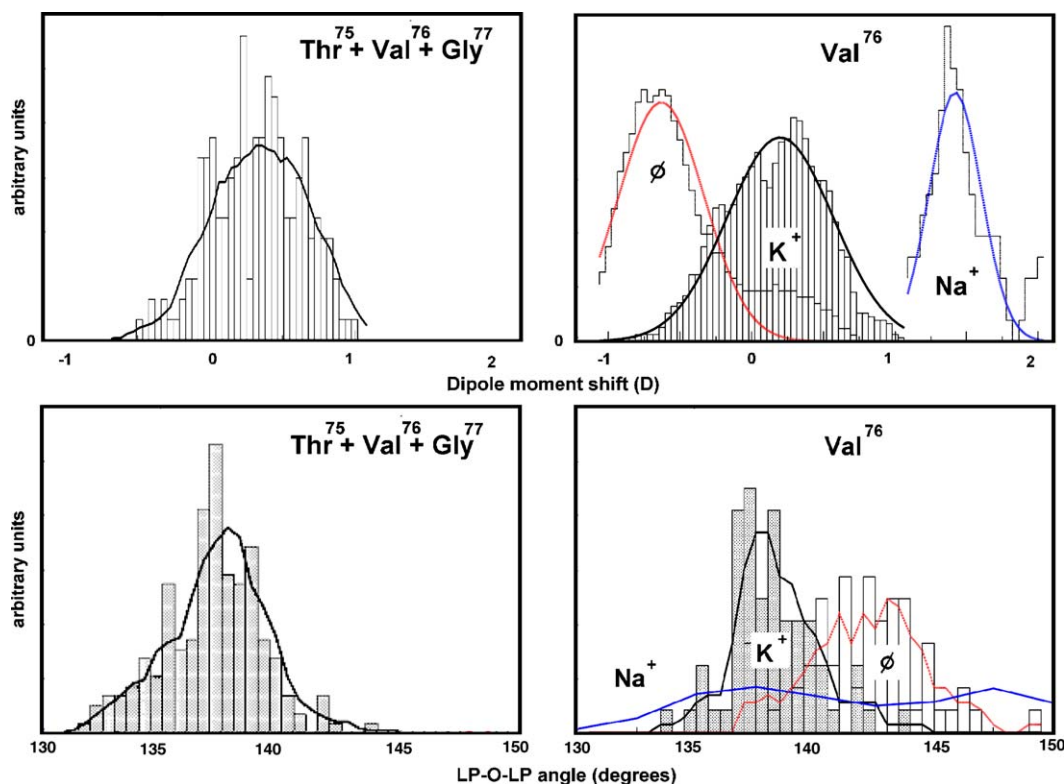


Fig. 3. Top panels: distribution of the selectivity filter carbonyl local dipole moments (formamide in vacuo is taken as reference); on the right, Val-76 ring carbonyl dipole moments with  $K^+$  at  $S_3$  ( $K^+$  band), with  $K^+$  replaced by  $Na^+$  at  $S_3$  ( $Na^+$  band), and with an empty  $S_3$  site ( $\emptyset$  band). Bottom: distribution of the angle LP-O-LP defined by the carbonyl oxygen lone pairs center of charge and the oxygen atom (see also Fig. 5).

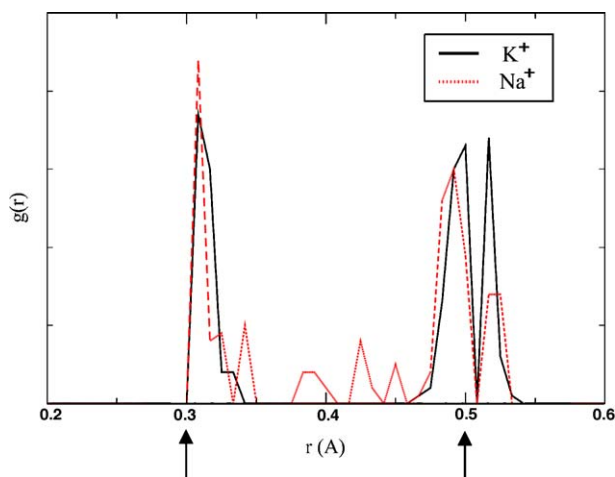


Fig. 4. Pair correlation function of the Wannier functions center of charge (WFCs) to the carbonyl oxygens for the oxygen lone pairs (peaks at 0.3 Å) and the  $\sigma$  and  $\pi$  bonds of the C=O groups (peaks at 0.5 Å). Solid line:  $K^+$  at site  $S_3$ ; dashed line:  $Na^+$  at site  $S_3$ ; arrows: position of the WFCs in formamide in the gas phase.

induced by the cation than the more straightforward comparison with formamide in vacuo indicates. The large  $K^+$  cation in the selectivity filter is also strongly polarized because of the slight asymmetry of the binding sites. As a consequence it bears a net dipole moment of  $0.31 \pm 0.09$  D, which does not significantly

depend on the specific binding site. Also the water molecule in  $S_2$  is largely polarized with an average dipole moment of  $2.49 \pm 0.19$  D to be compared to the gas phase value of 1.8 D. However, the water dipole moment in the channel is significantly smaller than that calculated at the same level of theory [65] for bulk water (3.0 D). This observation is likely a consequence of the small electric field exerted on the water at the  $S_2$  site possibly caused, at least in part, by the opposing fields created by the two cations.

In order to better understand the rearrangement of the electronic structure of the channel backbone in the presence of the cations, we have determined the center of charge of the corresponding Wannier functions [56]. The WO's, which are the analogue of Boys localized orbitals in a periodic system, allow the total charge to be partitioned, in a chemically transparent and unambiguous way, in doubly occupied orbitals associated with individual chemical contributions (such as covalent bonds and lone pairs). They therefore provide a useful tool for analyzing the change induced in the electronic structure. The information obtained might also be helpful for the design of new empirical force fields. We focus mainly on the displacement of the  $\sigma$  and  $\pi$  bonds of the C=O groups and of the lone pairs of the carbonyl oxygen atoms. As done for the analysis of the dipole moments, the electronic structure of the filter in the presence of the ions has been compared to the corresponding

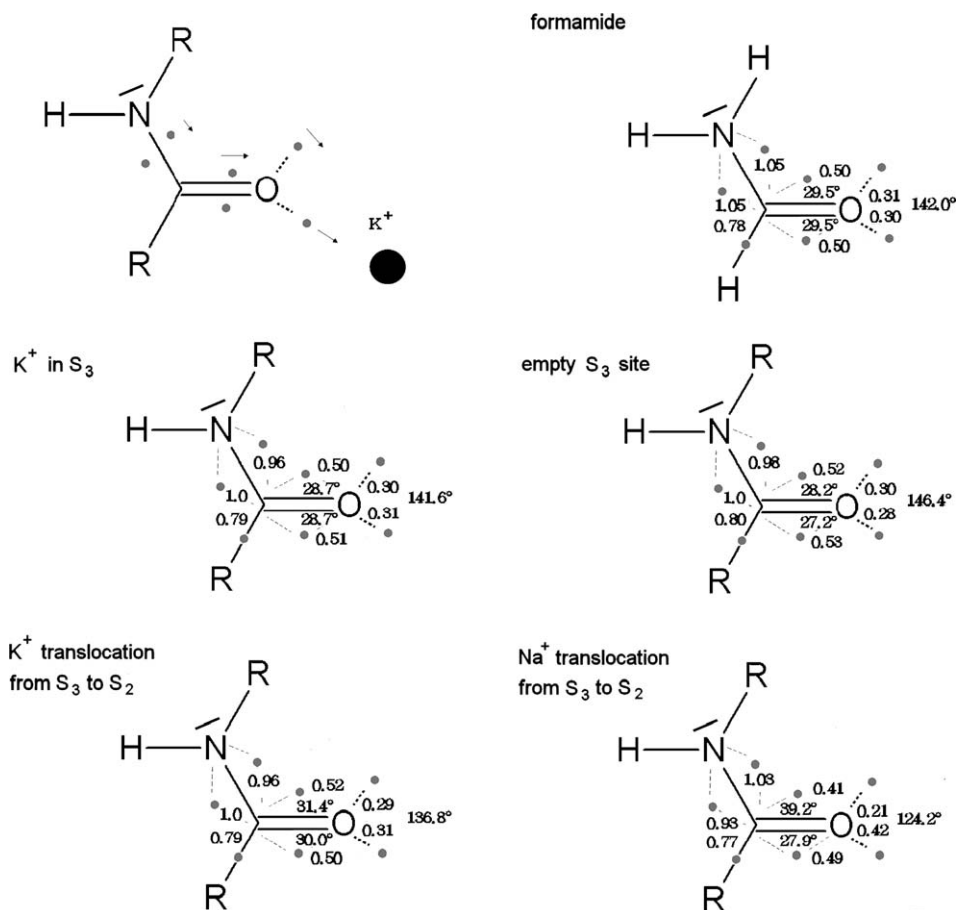


Fig. 5. Illustration of the Wannier Function Centers (WFCs) positions on the Val-76 ligands of the filter. Comparison between  $K^+$  and  $Na^+$  occupancy of the  $S_3$  binding site for the selectivity filter in the (1011) state. The distance in Å between atoms and the WFCs are displayed as well as the angles (in degrees) between the WFCs and the bonds axes.

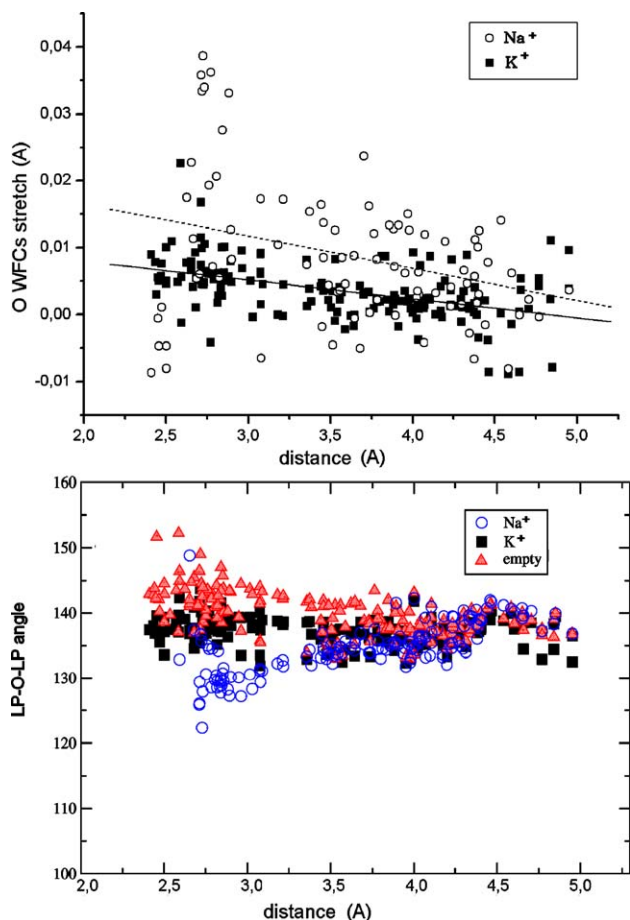


Fig. 6. Effect of the cation at  $S_3$  on the oxygen lone pairs of the carbonyl groups as a function of the metal–oxygen distance. Top: Displacement of the position (upper panel) and the bending angle between the oxygen lone pairs and the oxygen atom (lower panel). The values reported are relative to the empty  $S_3$  site.

reference state in which the middle  $K^+$  ion was removed while leaving all of the other atoms fixed. The results are analyzed in terms of pair correlation functions of the WFCs distribution around the carbonyl oxygens (Fig. 4). The displacement of the WFCs positions is of the order of  $5\text{--}10 \times 10^{-3}$  Å for lone pairs of the adjacent Val-76 carbonyl ring oxygens and of  $1\text{--}3 \times 10^{-3}$  Å for the lone pairs of the other neighboring carbonyl rings. The displacements relative to the  $C=O$  bond orbitals are found to be one order of magnitude larger. The angle between the WFCs oxygen lone pairs and the oxygen atom is particularly sensitive to the presence of the cation as reported in Fig. 3 (bottom). Similar computations were performed with the  $Na^+$  ion in place of the middle  $K^+$  ion. The displacement of the  $C=O$  bond orbitals and of the oxygen lone pairs is found to be twice as large as for  $K^+$  (Fig. 4), whereas the bend of the lone pair–oxygen lone pair angle is three times larger (Fig. 3, bottom). Fluctuations in the WFCs displacements also indicate a strong dependence of the polarization effects on the ion protein binding geometry. In some cases, the displacement of the  $C=O$  bond orbitals and of the oxygen lone pairs is found to be one order of magnitude larger than for the  $K^+$  ion (Fig. 4). The relative position of the WFCs with respect to reference atoms is shown in more details in Fig. 5 for a selected snapshot. As can

be seen, the carbonyl–cation interaction breaks the symmetry of the oxygen lone pairs. The electrostatic polarization of the  $C=O$  bond and  $C-N$  peptidic bond is equally evident. Polarization effects however do not extend to more than  $6\text{--}7$  Å away from the ion and they fall off almost linearly with distance (Fig. 6).

During the decay process from the state (1011) to the state (0101), the local dipole moment on the carbonyl groups undergoes a small, but significant, change. In Fig. 2b, the local dipole moments on the closest carbonyls to the  $K^+$  at  $S_3$  are reported. As the  $K^+$  cation at  $S_3$  gets closer to the Gly77 ring and further apart from the Thr75 ring the carbonyl dipole moment of the former increases, while the one of the latter appreciably decreases. The Val76 ring carbonyl dipole moments change less and they are always quite large because of the vicinity to the cation.

### 3.3. Charge transfer

The analysis of the polarization within the selectivity filter is based on the assumption that no charge transfer between the constituting units occurs. However, in a previous study on charge transfer at the solute/solvent interface [38], it was found that cations, which do not form hydrogen-bonds with the solvent, withdraw a small, but significant, fraction of electronic charge from the solvent, and give rise to a pure electrostatic polarization of the solvating water molecules. The net electronic charge transferred from water to the cation is  $0.13(2)e$  and  $0.12(2)e$  for  $K^+$  and  $Na^+$  cations, which means that a single solvating water molecule is responsible for charge transfer of about  $0.016e$  in case of  $K^+$  and  $0.020e$  in case of  $Na^+$ . Here, we have performed an AIM analysis of the electronic density of the selectivity filter. We have found that the  $K^+$  in the potassium channel withdraws approximately the same amount of charge from the surrounding carbonyl groups. The net ionic charge however depends distinctly on the binding site. The cation

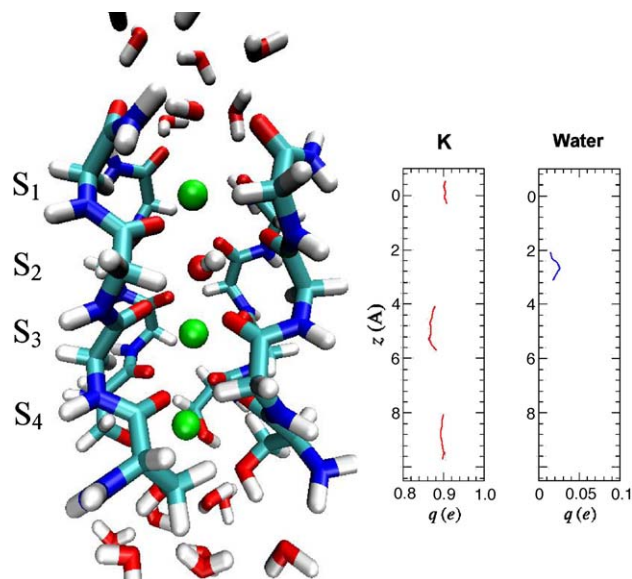


Fig. 7. Decay process from the (1011) to the (0101) state. Net charge on the cation and on the inner water molecule as a function of the  $z$ -coordinate.

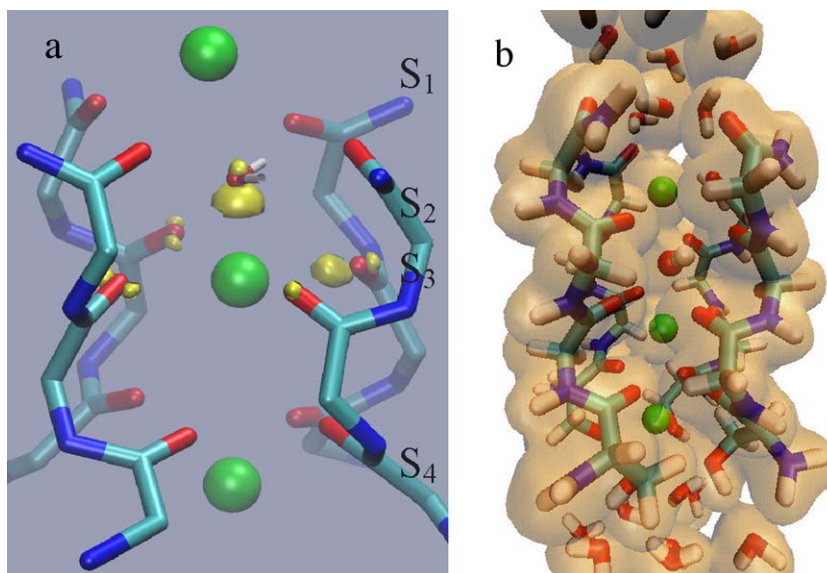


Fig. 8. Selectivity filter in the (1011) state. (a) Density difference induced by the middle  $K^+$  cation for an isovalue of  $2 \times 10^{-3}e$ ; (b) Isosurface enclosing the 95% of the total density.

located at the site  $S_3$  has a net charge of  $+0.87e$ , which is slightly smaller than that of the cations in the binding sites  $S_1$  [and  $S_4$  in the case of the (1011) state], which have net charges of  $+0.90e$ . The same picture is obtained when  $K^+$  is replaced by  $Na^+$ . The water in the binding site  $S_2$  has a net positive charge of  $+0.015e$ . This water is not properly oriented to interact with the cations (the plane of the molecule is nearly perpendicular to the  $O_{\text{wat}}-K^+$  axis) and transfers charge mainly to the filter backbone trough H-bonding. The net charge on the cations and the water molecule during the evolution of the (1011) state is reported in Fig. 7.

The nature of the charge transfer between  $K^+$  and the channel as well as the magnitude of the energies due to polarization effects can be further rationalized by studying a simple system where a metal cation is coordinated to 8 formaldehyde molecules, which can be considered as a minimal model of the  $S_2$  and  $S_3$  binding sites. Calculations were performed at both DFT/BLYP and DFT/B3LYP level of theory using 6-311++G(3dp,2p) Gaussian basis sets and the donor–acceptor interactions were analyzed within the Natural Bond Orbital (NBO) scheme [66]. A large  $\sigma(\text{CO}) \rightarrow s(K^+)$  and  $n(\text{CO}) \rightarrow p(K^+)$  charge transfer is observed. The metal mainly receives charge in the valence orbitals. In contrast, the charge transferred from the cation toward the carbonyls is negligible. The amount of charge transferred at the minimum energy configuration is about 0.06e and 0.1 for  $K^+$  and  $Na^+$ , respectively. These values nicely compare with the charge transfer calculated for the metal ion in the selectivity filter. According to the NBO perturbative framework [66], the donor–acceptor interaction energy due to the charge transfer is higher for  $Na^+$  than for  $K^+$  ( $\Delta E_{\text{CT}} = -17 \text{ kcal/mol}$ ). In contrast, the intramolecular energy stabilization due to polarization effects is only slightly larger for  $Na^+$  than for  $K^+$  ( $\Delta E_{\text{CT}} = -1 \text{ kcal/mol}$ ). It is important to remark that inside the channel the stabilization energy of the metal ion due to

the polarization would be larger. On the basis of this simple model of the binding site, however, it emerges that charge transfer may play an important role in stabilizing the cations in the selectivity filter.

#### 4. Discussion

The present calculations suggest that the presence of the cations causes large distortions of the channel electronic density that are due to polarization effects. This can be seen in Fig. 8a, where the electronic density difference between the channel with  $K^+$  in  $S_3$  and the density with the empty  $S_3$  site is reported. The large differences in the  $K^+$  and  $Na^+$  calculated average induced dipoles (about  $+0.2\text{D}$  and  $+1.5\text{D}$  for  $K^+$  and  $Na^+$ , respectively) might have a direct influence on the selectivity mechanism. In a recent study, Noskov et al. [64] have demonstrated that by removing the carbonyl–carbonyl interaction in the  $S_2$  binding site of a fully flexible KcsA channel, the selectivity for  $K^+$  over  $Na^+$  was annihilated. These findings led the authors to propose that the carbonyl–carbonyl repulsion has little effect on the pore radius, but plays a key role for the ion-binding energetics [64]. This mechanism may explain why the selectivity is not affected by thermal fluctuations, which destroy the sub-angstrom fine structure of the selectivity filter. Similarly, we found that the inclusion of induced polarization effects can influence the ion-binding energetics without triggering any major geometrical change. A simple electrostatic calculation done on a model with 8 carbonyls, representing two adjacent  $\text{C}=\text{O}$  ring of the filter, shows that increasing the charge on the oxygen ligands by  $0.2e$  with an accompanying dipole change of  $\sim 1.2\text{D}$ , results in a total repulsion energy of several tens of kcal/mol. Considering that the interaction energy between the ion and its surrounding does not differ significantly between  $K^+$  and  $Na^+$  [64], the large polarization of carbonyl groups by

the Na<sup>+</sup> ion could generate a repulsion energy sufficient to favor K<sup>+</sup> binding over Na<sup>+</sup>.

Besides polarization effects also charge transfer should be considered when discussing the permeation mechanism in KcsA K<sup>+</sup> channel. This effect is caused by a significant overlap between wave functions associated with the ions and the protein backbone, as can be seen in Fig. 8b, where an isosurface enclosing 95% of the total density is reported. Thus, our calculations reveal a large charge transfer from the selectivity filter backbone to the cations. One direct consequence of this effect can be the screening of the ion–ion repulsion, which can influence the coupled movement of ions inside the selectivity filter and therefore the ion conduction pathways. The concept of coupled ion movement, in which two ions and two water molecules move through the pore in a concerted manner, was introduced by Hodgkin and Keynes [8] and later confirmed by MD simulations on ion conduction through KcsA [11,67]. Our analysis on charge transfer in the formaldehyde cluster model suggests that the screening of the ion–ion repulsion in KcsA, for ions located in S<sub>1</sub> and S<sub>3</sub>, is larger for Na<sup>+</sup> than for K<sup>+</sup> ( $\Delta E_{CT}=4$  kcal/mol using a simple Coulomb law). We conclude remarking that, although it might be possible that charge transfer plays a role in the multi-ion conduction, it is not expected to appreciably influence the observed high selectivity for K<sup>+</sup> over Na<sup>+</sup> as some recent simulations suggest [68].

## 5. Conclusions

Our QM/MM calculations show that the cations in the selectivity filter induce a large electronic polarization of the carbonyl groups and a sizable charge transfer from the carbonyl groups to the cations. Induced polarization is relatively short-ranged and negligible at distances larger than 7–8 Å. These effects are more pronounced for Na<sup>+</sup> than for K<sup>+</sup> and are also strongly directional: an ion approaching parallel or perpendicular to the lone pair orbitals induces different polarization and charge transfer. Although our calculations do not systematically cover a complete investigation of all possible ionic loading states in the filter, they suggest that polarization [15] and charge transfer effects [38] may play a role in the conduction and/or the selectivity mechanism of the KcsA K<sup>+</sup> channel and other K<sup>+</sup> channels, and offer to the next generation of intermolecular (polarizable) force fields the challenge to correctly describe charge transfer processes [33].

## References

- [1] F.M. Ashcroft, *Ion Channels and Disease*, Academic Press, San Diego, 2000.
- [2] B. Hille, *Ionic Channels of Excitable Membranes* Sinauer Associates, Sunderland, Massachusetts, 2001.
- [3] R. MacKinnon, Nobel lecture. Potassium channels and the atomic basis of selective ion conduction, *Bioscience Reports* (2004).
- [4] J.H. Morais-Cabral, Y.F. Zhou, R. MacKinnon, Energetic optimization of ion conduction rate by the K<sup>+</sup> selectivity filter, *Nature* 414 (2001) 37–42.
- [5] R.T. Shealy, A.D. Murphy, R. Ramarathnam, E. Jakobsson, S. Subramaniam, *Biophysical Journal* 84 (2003) 2929–2942.
- [6] R. MacKinnon, S.L. Cohen, A.L. Kuo, A. Lee, B.T. Chait, Structural conservation in prokaryotic and eukaryotic potassium channels, *Science* 280 (1998) 106–109.
- [7] S.B. Long, E.B. Campbell, R. MacKinnon, Crystal structure of a mammalian voltage-dependent Shaker family K<sup>+</sup> channel, *Science* 309 (2005) 897–903.
- [8] A.L. Hodgkin, R.D. Keynes, The potassium permeability of a giant nerve fibre, *Journal of Physiology (London)* 128 (1955) 61–88.
- [9] M. LeMasurier, L. Heginbotham, C. Miller, KcsA: it's a potassium channel, *Journal of General Physiology* 118 (2001) 303–313.
- [10] C. Alcayaga, X. Cecchi, O. Alvarez, R. Latorre, Streaming potential measurements in Ca<sup>2+</sup>-activated K<sup>+</sup> channels from skeletal and smooth-muscle-coupling of ion and water fluxes, *Biophysical Journal* 55 (1989) 367–371.
- [11] J. Aqvist, V. Luzhkov, Ion permeation mechanism of the potassium channel, *Nature* 404 (2000) 881–884.
- [12] S. Berneche, B. Roux, Energetics of ion conduction through the K<sup>+</sup> channel, *Nature* 414 (2001) 73–77.
- [13] S. Berneche, B. Roux, Molecular dynamics of the KcsA K<sup>+</sup> channel in a bilayer membrane, *Biophysical Journal* 78 (2000) 2900–2917.
- [14] L. Guidoni, V. Torre, P. Carloni, Water and potassium dynamics inside the KcsA K<sup>+</sup> channel, *FEBS Letters* 477 (2000) 37–42.
- [15] L. Guidoni, V. Torre, P. Carloni, Potassium and sodium binding to the outer mouth of the K<sup>+</sup> channel, *Biochemistry* 38 (1999) 8599–8604.
- [16] M.S.P. Sansom, I.H. Shrivastava, R.J. Law, C.E. Capener, Simulations of potassium channel function: KcsA and homology models, *Journal of General Physiology* 116 (2000) 27A.
- [17] P.C. Biggin, G.R. Smith, I. Shrivastava, S. Choe, M.S.P. Sansom, Potassium and sodium ions in a potassium channel studied by molecular dynamics simulations, *Biochimica et Biophysica Acta. Biomembranes* 1510 (2001) 1–9.
- [18] V.B. Luzhkov, J. Aqvist, Ions and blockers in potassium channels: insights from free energy simulations, *Biochimica et Biophysica Acta. Proteins and Proteomics* 1747 (2005) 109–120.
- [19] V.B. Luzhkov, J. Aqvist, K<sup>+</sup>/Na<sup>+</sup> selectivity of the KcsA potassium channel from microscopic free energy perturbation calculations, *Biochimica et Biophysica Acta-Protein Structure and Molecular Enzymology* 1548 (2001) 194–202.
- [20] T.W. Allen, S. Kuyucak, S.H. Chung, Molecular dynamics study of the KcsA potassium channel, *Biophysical Journal* 77 (1999) 2502–2516.
- [21] J. Neyton, C. Miller, Discrete Ba<sup>2+</sup> block as a probe of ion occupancy and pore structure in the high-conductance Ca<sup>2+</sup>-activated K<sup>+</sup> channel, *Journal of General Physiology* 92 (1988) 569–586.
- [22] C.M. Nimigean, C. Miller, Na<sup>+</sup> block and permeation in a K<sup>+</sup> channel of known structure, *Journal of General Physiology* 120 (2002) 323–335.
- [23] B. Roux, Ion conduction and selectivity in K<sup>+</sup> channels, *Annual Review of Biophysics and Biomolecular Structure* 34 (2005) 153–171.
- [24] B. Roux, T. Allen, S. Berneche, W. Im, Theoretical and computational models of biological ion channels, *Quarterly Reviews of Biophysics* 37 (2004) 15–103.
- [25] B. Roux, S. Berneche, On the potential functions used in molecular dynamics simulations of ion channels, *Biophysical Journal* 82 (2002) 1681–1684.
- [26] T.A. Halgren, W. Damm, Polarizable force fields, *Current Opinion in Structural Biology* 11 (2001) 236–242.
- [27] M.B. Partenskii, P.C. Jordan, Nonlinear dielectric behavior of water in transmembrane ion channels—ion energy barriers and the channel dielectric constant, *Journal of Physical Chemistry* 96 (1992) 3906–3910.
- [28] T.W. Allen, S.H. Chung, S. Kuyucak, Molecular and Brownian dynamics of the potassium channel, *Biophysical Journal* 80 (2001) 328A.
- [29] D.P. Tieleman, P.C. Biggin, G.R. Smith, M.S.P. Sansom, Simulation approaches to ion channel structure–function relationships, *Quarterly Reviews of Biophysics* 34 (2001) 473–561.
- [30] P. Cieplak, J. Caldwell, P. Kollman, Molecular mechanical models for organic and biological systems going beyond the atom centered two body additive approximation: Aqueous solution free energies of methanol and *N*-methyl acetamide, nucleic acid base, and amide hydrogen bonding and chloroform/water partition coefficients of the nucleic acid bases, *Journal of Computational Chemistry* 22 (2001) 1048–1057.

- [31] A. Grossfield, P.Y. Ren, J.W. Ponder, Ion solvation thermodynamics from simulation with a polarizable force field, *Journal of the American Chemical Society* 125 (2003) 15671–15682.
- [32] G.A. Kaminski, H.A. Stern, J.L. Banks, R.H. Zhou, R.A. Friesner, B.J. Berne, Ab initio derived force field for biomolecular applications with explicit treatment of electrostatic polarizability, *Abstracts of Papers of the American Chemical Society* 218 (1999) U503–U504.
- [33] G.A. Kaminski, H.A. Stern, B.J. Berne, R.A. Friesner, Development of an accurate and robust polarizable molecular mechanics force field from ab initio quantum chemistry, *Journal of Physical Chemistry A* 108 (2004) 621–627.
- [34] G.A. Kaminski, H.A. Stern, B.J. Berne, R.A. Friesner, Y.X.X. Cao, R.B. Murphy, R.H. Zhou, T.A. Halgren, Development of a polarizable force field for proteins via ab initio quantum chemistry: first generation model and gas phase tests, *Journal of Computational Chemistry* 23 (2002) 1515–1531.
- [35] S. Patel, A.D. Mackerell, C.L. Brooks, CHARMM fluctuating charge force field for proteins: II—Protein/solvent properties from molecular dynamics simulations using a nonadditive electrostatic model, *Journal of Computational Chemistry* 25 (2004) 1504–1514.
- [36] P.Y. Ren, J.W. Ponder, Consistent treatment of inter- and intramolecular polarization in molecular mechanics calculations, *Journal of Computational Chemistry* 23 (2002) 1497–1506.
- [37] H.A. Stern, G.A. Kaminski, J.L. Banks, R.H. Zhou, B.J. Berne, R.A. Friesner, Fluctuating charge, polarizable dipole, and combined models: parameterization from ab initio quantum chemistry, *Journal of Physical Chemistry B* 103 (1999) 4730–4737.
- [38] M. Dal Peraro, S. Raugei, P. Carloni, M.L. Klein, Solute–solvent charge transfer in aqueous solution, *Chemical Physics and Physical Chemistry* 6 (2005) 1719.
- [39] L. Guidoni, P. Carloni, Potassium permeation through the KcsA channel: a density functional study, *Biochimica et Biophysica Acta. Biomembranes* 1563 (2002) 1–6.
- [40] W. Kohn, L.J. Sham, Self-consistent equations including exchange and correlation effects, *Physical Review* 140 (1965) 1133.
- [41] Y.F. Zhou, J.H. Morais-Cabral, A. Kaufman, R. MacKinnon, Chemistry of ion coordination and hydration revealed by a K<sup>+</sup> channel–Fab complex at 2.0 angstrom resolution, *Nature* 414 (2001) 43–48.
- [42] Q.F. Zhong, Q. Jiang, P.B. Moore, D.M. Newns, M.L. Klein, Molecular dynamics simulation of a synthetic ion channel, *Biophysical Journal* 74 (1998) 3–10.
- [43] D.C.J.M. Doyle, R.A. Pfuetzner, A. Kuo, J.M. Gulbis, S.L. Cohen, B.T. Chait, R. MacKinnon, The structure of the potassium channel: molecular basis of K<sup>+</sup> conduction and selectivity, *Science* 280 (1998) 69–77.
- [44] A. Gross, L. Columbus, K. Hideg, C. Altenbach, W.L. Hubbell, Structure of the KcsA potassium channel from *Streptomyces lividans*: A site-directed spin labeling study of the second transmembrane segment, *Biochemistry* 38 (1999) 10324–10335.
- [45] J.M. Wang, R.M. Wolf, J.W. Caldwell, P.A. Kollman, D.A. Case, Development and testing of a general amber force field, *Journal of Computational Chemistry* 25 (2004) 1157–1174.
- [46] T. Darden, D. York, L. Pedersen, Particle Mesh Ewald—an N.Log(N) method for Ewald Sums in large systems, *Journal of Chemical Physics* 98 (1993) 10089–10092.
- [47] C. Domene, M.S.P. Sansom, Potassium channel, ions, and water: simulation studies based on the high resolution X-ray structure of KcsA, *Biophysical Journal* 85 (2003) 2787–2800.
- [48] Y.F. Zhou, R. MacKinnon, The occupancy of ions in the K<sup>+</sup> selectivity filter: charge balance and coupling of ion binding to a protein conformational change underlie high conduction rates, *Journal of Molecular Biology* 333 (2003) 965–975.
- [49] R. Car, M. Parrinello, Unified approach for molecular-dynamics and density-functional theory, *Physical Review Letters* 55 (1985) 2471–2474.
- [50] A. Laio, J. VandeVondele, U. Rothlisberger, A Hamiltonian electrostatic coupling scheme for hybrid Car–Parrinello molecular dynamics simulations, *Journal of Chemical Physics* 116 (2002) 6941–6947.
- [51] W. Kohn, A.D. Becke, R.G. Parr, Density functional theory of electronic structure, *Journal of Physical Chemistry* 100 (1996) 12974–12980.
- [52] C.T. Lee, W.T. Yang, R.G. Parr, Development of the Colle–Salvetti correlation-energy formula into a functional of the electron-density, *Physical Review. B* 37 (1988) 785–789.
- [53] N.M.J. Trouiller, *Physical Review. B* 43 (1993).
- [54] S. Nose, A unified formulation of the constant temperature for molecular dynamics methods, *Journal of Chemical Physics* 84 (1984) 511–519.
- [55] W. Hoover, Canonical dynamics: equilibrium phase-space distributions, *Physical Review. A* 31 (1985) 1695–1697.
- [56] P.L. Silvestrelli, N. Marzari, D. Vanderbilt, M. Parrinello, Maximally-localized Wannier functions for disordered systems: application to amorphous silicon, *Solid State Communications* 107 (1998) 7–11.
- [57] R.F.W. Bader, *Atoms in Molecules. A Quantum Theory*, vol. 22, Oxford University Press, Oxford, 1990.
- [58] B. Szeferczyk, W.A. Sokalski, J. Leszczynski, *Journal of Chemical Physics* 117 (2002) 6952.
- [59] D.S. Kosov, P.L.A. Popelier, *Journal of Chemical Physics* 104 (2000) 3969.
- [60] P.L.A. Popelier, L. Joubert, D.S. Kosov, *Journal of Physical Chemistry. A* 105 (2000) 8254.
- [61] W.A. Sokalski, *Journal of Chemical Physics* 77 (1982) 4529.
- [62] Y. Zhou, R. MacKinnon, Ion binding affinity in the cavity of the KcsA potassium channel, *Biochemistry* 43 (2004) 4978–4982.
- [63] I.H. Shrivastava, D.P. Tieleman, P.C. Biggin, M.S.P. Sansom, K<sup>+</sup> versus Na<sup>+</sup> ions in a K channel selectivity filter: a simulation study, *Biophysical Journal* 83 (2002) 633–645.
- [64] S.Y. Noskov, S. Berneche, B. Roux, Control of ion selectivity in potassium channels by electrostatic and dynamic properties of carbonyl ligands, *Nature* 431 (2004) 830–834.
- [65] P.L. Silvestrelli, M. Parrinello, Water molecule dipole in the gas and in the liquid phase, *Physical Review Letters* 82 (1999) 3308–3311.
- [66] J. Foster, F. Weinhold, *Journal of American Chemistry and Society* 102 (1980) 7211.
- [67] S. Berneche, B. Roux, Free energy profile and correlated translocation of ions in the KcsA potassium channel, *Biophysical Journal* 78 (2000) 17A.
- [68] A. Burykin, M. Kato, A. Warshel, Exploring the origin of the ion selectivity of the KcsA potassium channel, *Proteins, Structure, Function, and Genetics* 52 (2003) 412–426.
- [69] B. Roux, M. Karplus, Potential-energy function for cation-peptide interactions—an ab-initio study, *Journal of Computational Chemistry* 16 (1995) 690–704.
- [70] I.H. Shrivastava, M.S.P. Sansom, Simulations of ion permeation through a potassium channel: molecular dynamics of KcsA in a phospholipid bilayer, *Biophysical Journal* 78 (2000) 557–570.
- [71] I. Dzidic, P. Kebarle, Hydration of Alkali Ions in Gas Phase—Enthalpies and Entropies of Reactions  $M^+(H_2O)_{n-1} + H_2O = M^+(H_2O)_n$ , *Journal of Physical Chemistry* 74 (1970) 1466.
- [72] J.S. Klassen, S.G. Anderson, A.T. Blades, P. Kebarle, Reaction enthalpies for  $M^+L = M^+ + L$ , where  $M^+ = Na^+$  and  $K^+$  and L equals acetamide, *N*-methylacetamide, *N,N*-dimethylacetamide, glycine, and glycylglycine, from determinations of the collision-induced dissociation thresholds, *Journal of Physical Chemistry* 100 (1996) 14218–14227.
- [73] T.W. Allen, A. Bliznyuk, A.P. Rendell, S. Kuyucak, S.-H. Chung, The potassium channel: structure, selectivity and diffusion, *Journal of Chemical Physics* 112 (2000) 8191–8204.